



Translational Model-Informed Approach for Selection of Tuberculosis Drug Combination Regimens in Early Clinical Development

Budi O. Susanto¹, Sebastian G. Wicha², Yanmin Hu³, Anthony R.M. Coates³ and Ulrika S.H. Simonsson^{1,*}

The development of optimal treatment regimens in tuberculosis (TB) remains challenging due to the need of combination therapy and possibility of pharmacodynamic (PD) interactions. Preclinical information about PD interactions needs to be used more optimally when designing early bactericidal activity (EBA) studies. In this work, we developed a translational approach which can allow for forward translation to predict efficacy of drug combination in EBA studies using the Multistate Tuberculosis Pharmacometric (MTP) and the General Pharmacodynamic Interaction (GPDI) models informed by *in vitro* static time-kill data. These models were linked with translational factors to account for differences between the *in vitro* system and humans. Our translational MTP-GPDI model approach was able to predict the EBA_{0–2 days}, EBA_{0–5 days}, and EBA_{0–14 days} from different EBA studies of rifampicin and isoniazid in monotherapy and combination. Our translational model approach can contribute to an optimal dose selection of drug combinations in early TB clinical trials.

Study Highlights

WHAT IS THE CURRENT KNOWLEDGE ON THE TOPIC?

✓ Typical early bactericidal activity (EBA) studies of antituberculosis drugs are mostly performed in monotherapy, which are later tested in combination for longer treatment outcomes in phase IIb trials.

WHAT QUESTION DID THIS STUDY ADDRESS?

✓ How to inform dose selection of antituberculosis drug combinations for planning EBA studies using a translational model-informed approach to better exploit preclinical *in vitro* information.

WHAT DOES THIS STUDY ADD TO OUR KNOWLEDGE?

✓ The *in vitro*-based translational approach successfully predicted different observed EBA studies of isoniazid and

rifampicin in monotherapy as well as in combination. The approach was not only able to support dose selection but also to identify the pharmacodynamics interaction of the combination.

HOW MIGHT THIS CHANGE CLINICAL PHARMACOLOGY OR TRANSLATIONAL SCIENCE?

✓ Our approach encourages evaluating drug combinations early in phase IIa trials instead of only testing monotherapy and can be used to support dose selection of drug combinations using *in vitro* combination data.

A more effective regimen with a shorter treatment duration is an urgent need to provide more efficient treatment options for patients with pulmonary tuberculosis (TB). Since TB treatment requires multidrug regimens, pharmacodynamics (PD) interactions can be a challenge for developing optimal regimens. The typical early bactericidal activity (EBA) study in a TB phase IIa trial acts as the first “proof-of-concept” study of microbiological activity in humans when the drug is given as monotherapy for 2 weeks. Few EBA studies have explored combinations of drugs,^{1,2} but traditionally the EBA studies have played a role in dose selection for the phase IIb trials where the results from the EBA study informs the combination regimen to be

evaluated. However, the most optimal dose in monotherapy may not be the optimal dose for combination treatment. Therefore, it is not possible to study the most optimal dose combinations in humans due to the many possible combinations. An alternative is to use preclinical *in vitro* information where it is possible to study a large set of combinations in order to define the PD interaction space. However, prediction of clinical efficacy based on *in vitro* information needs to account for translational factors such as human pharmacokinetics (PK), target site exposure, and mycobacterial factors, such as bacterial growth phase, postantibiotic effect (PAE), and minimum inhibitory concentration (MIC) distribution.³

¹Department of Pharmaceutical Biosciences, Uppsala University, Uppsala, Sweden; ²Department of Clinical Pharmacy, Institute of Pharmacy, University of Hamburg, Hamburg, Germany; ³Institute for Infection and Immunity, St. George's University of London, London, UK. *Correspondence: Ulrika S.H. Simonsson (ulrika.simonsson@farmbio.uu.se)

Received August 30, 2019; accepted February 8, 2020. doi:10.1002/cpt.1814

The General Pharmacodynamic Interaction (GPDI) model is a novel model-based assessment approach for quantifying PD interactions,⁴ which has successfully been combined with the Multistate Tuberculosis Pharmacometric (MTP) model,⁵ a semimechanistic model developed to characterize drug effects on different growth states of the TB bacterium. The MTP-GPDI approach has been used to identify PD interactions both *in vitro*⁶ and *in vivo*⁷ and has been shown to be superior compared with other approaches for identifying PD interactions.⁸ A forward translation framework for clinical exposure–response forecasting in EBA studies based on preclinical *in vitro* information using the MTP model has been successfully developed for rifampicin.³ In this work, we developed a translational approach which allows for forward translation to extend the framework to predict the efficacy of the drug combination in EBA studies. This approach accounted for PD interactions which were identified *in vitro* using the MTP-GPDI model for rifampicin and isoniazid combination as an example.

MATERIALS AND METHODS

In vitro preclinical data

The following procedures were performed to obtain natural growth data. *Mycobacterium tuberculosis* strain H37Rv was grown in serial of 10 mL 7H9 medium containing 0.05% Tween 80 supplemented with 10% albumin dextrose complex (ADC; Becton and Dickinson, Oxford, UK) at 37°C without disturbance for 100 days. The colony-forming unit (CFU) counts were performed by plating a serial of 10-fold dilutions of the cultures on 7H11 agar medium supplemented with oleic albumin dextrose complex (OADC; Becton and Dickinson). The 7H11 agar plates were made according to the manufacturer's instructions. Colonies were counted after incubation of the plates at 37°C for 3–4 weeks and viability was expressed as log CFU/mL.

In vitro static time-kill curve data was obtained from log-phase *M. tuberculosis* H37Rv (4-day-old culture) exposed to isoniazid at 0–16 mg/L at 37°C and stationary-phase *M. tuberculosis* H37Rv (100-day-old culture) exposed to isoniazid at 0–64 mg/L at 37°C (Figure S1). For isoniazid-rifampicin combination, only static time-kill assays in stationary-phase were available. The bacteria were exposed to different concentrations of isoniazid-rifampicin combination at 0–64 mg/L for each drug (Figure S2). The drug concentration/stability was not measured during the whole experiment. During the model-building process, *in vitro* data for rifampicin in monotherapy⁵ and isoniazid in monotherapy were pooled with isoniazid-rifampicin combination data. The CFU was used as a biomarker which represents the number of viable bacteria in the sample. For isoniazid monotherapy, the CFU was observed at time 0, 4, 6, 9, 14, 24, and 34 days for log-phase and at time 100, 103, 108, 116, 120, and 124 days for stationary-phase. For isoniazid-rifampicin combination, the CFU was counted at time 100, 103, 106, 110, and 114 days. Each observation had one replicate. All work on *M. tuberculosis* was performed in a Class I Biosafety cabinet of Containment Level 3 Laboratory at St George's University of London.

In vitro exposure–response relationships of isoniazid and rifampicin in monotherapy

The MTP model was applied to log-phase and stationary-phase data to describe the exposure–response relationship of isoniazid and rifampicin monotherapy *in vitro*. The MTP model assumed three bacterial states: fast-multiplying (*F*), slow-multiplying (*S*), and nonmultiplying (*N*) state mycobacteria and how each mycobacterial state transferred to other states.⁵ The bacterial change was quantified using CFU, and

the CFU was assumed to be the sum of *F* and *S* states. No individual *in vitro* experiments were conducted using only *F* and *S* experiments. All CFU data were transformed into natural logarithms during the model-building process. All natural growth parameters were fixed to the same value as reported in the original MTP model.⁵ Reestimation of the natural growth parameters was done, but it was not statistically significant. Therefore, natural growth parameters were fixed in order to facilitate the identification of the exposure–response model parameters. The effect of isoniazid and rifampicin were tested towards four effect sites: *F* growth, killing of *F*, *S*, and *N* states. Exposure–response relationships of isoniazid at each effect site were evaluated using on/off effect, linear function, power function, E_{\max} function, and sigmoid E_{\max} function. The model was statistically significant if the objective function value (OFV) dropped at least 3.84 (χ^2 distribution, $\alpha < 0.05$) for nested models and for one parameter difference between the two models. All identified exposure–response relationships for each effect site were then combined and evaluated because drug effect may appear when the effect was combined with other effect sites. All possible combinations from previous steps were combined using at least a linear function. The best model from the previous step was chosen based on statistical significance ($\alpha < 0.05$). Reevaluation of the best model was done at each effect site by changing the effect function into a more complex model and a simpler model. The model with better fit to the data based on statistical significance was kept and carried forward to the next step. A final backward elimination was done by deleting one effect site at a time to exclude nonsignificant effect sites at 1% significant level.

In vitro exposure–response relationships of isoniazid and rifampicin in combination

The PD interactions in combination therapy were assessed using the GPDI model⁴ implemented in the Bliss Independence (BI) additivity criterion. All PD interactions were evaluated as a change in drug effect parameter (concentration of drug producing 50% of maximum effect (EC_{50}) or slope) which were parameterized by interaction (INT) parameter. Positive INT value indicates increase in EC_{50} or slope, i.e., antagonism, while the decrease in EC_{50} or slope, i.e., synergism, is expressed by INT between -1 and 0 . When there is no interaction, INT value will be zero, which is called "as expected additivity" to describe the total effect of both drugs. The potential PD interactions between isoniazid and rifampicin were characterized at each effect site.

During the evaluation of PD interactions, the natural growth parameters and final exposure–response parameters of isoniazid and rifampicin were fixed as identified in monotherapy. We evaluated the bidirectional interaction (isoniazid to rifampicin and vice versa) for each effect site. Then, the interaction at one effect site was combined with interactions at other effect sites one by one to the model. Only interactions that gave significant decrease in OFV ($\alpha < 0.05$) were kept and proceeded to the next step. Furthermore, to identify the interaction that was not significant in the best model in the previous step, each interaction parameter was removed one at a time. The final model was chosen based on the best fit of the model to the data from the previous step and the low uncertainty in parameter estimate.

Translational factors

To account for the different systems in *in vitro* experiments and in human, translational factors including PAE, mycobacterial susceptibility, bacterial growth phase, population pharmacokinetics, and epithelial lining fluid (ELF) model parameters were incorporated into the model.³ The bacteria in humans were assumed to grow for a 150-day period before treatment was started. PAE accounts for the suppression of bacterial growth after brief exposure to antibiotic.⁹ The PAE model for isoniazid was developed using an effect compartment model to link between isoniazid exposure and the MTP model developed for isoniazid monotherapy. Parameters for the PAE model were estimated from *in vitro* PAE observation of isoniazid.^{10,11} The

PAE model parameters for rifampicin were taken from a previous study.³ The PAE parameters for isoniazid-rifampicin combination were assumed to be the same as for monotherapy because there were not enough data in the literature to estimate the PAE parameter for the combination.

To characterize the different susceptibility of the bacteria *in vitro* and in human, MIC ratio was used to scale the drug concentration in target site (epithelial lining fluid). For *in vitro* MIC in *M. tuberculosis* H37Rv, we used the mode of MIC distribution for isoniazid¹² in order not to bias by choosing a single MIC value. For clinical MIC, the distribution from literature¹³ was used and random sampling was done to parameterize $MIC_{target}/MIC_{origin}$. To account for the change in drug concentration in humans, population PK models for rifampicin¹⁴ and isoniazid^{15,16} were incorporated into the model prediction. The ELF model parameters for isoniazid¹⁷ and rifampicin¹⁸ were also included into the prediction to account for the drug concentration in lung. The simulated drug concentration from the population PK model was fed into the plasma/ELF model and thereafter linked to the efficacy through the concentration-effect model which was identified using *in vitro* static concentration.

Clinical phase IIa EBA data

The clinical data were obtained by literature search from published EBA studies of isoniazid monotherapy and isoniazid-rifampicin combination available on PubMed using the words “early bactericidal activity isoniazid.” Only trials from drug-susceptible tuberculosis with CFU as bio-marker were included in our study.

Clinical phase IIa EBA trial simulation

The final MTP model *in vitro* and translational factors for isoniazid were implemented to simulate and predict clinical isoniazid EBA studies. The final MTP-GPDI model *in vitro* for isoniazid-rifampicin combination and translational factors for isoniazid and rifampicin monotherapy were used to simulate and predict the EBA studies of isoniazid-rifampicin combination. We performed 1,000 random sampling from log normal distribution for all PK variabilities and covariates. The observed EBA_{0–2 days}, EBA_{0–5 days}, and EBA_{0–14 days} from different EBA trials were compared with the model prediction to show the ability of the approach to predict clinical data based on *in vitro* data of efficacy.

Software

Modelling of *in vitro* data was performed with NONMEM (version 7.3; Icon Development Solutions (<https://www.iconplc.com/innovation/nonmem/>) Ellicott City, MD), using Laplacian conditional estimation with interaction. The M3 method¹⁹ was used to handle data below limit of quantification (LOQ) of 10 CFU/mL. The prediction-corrected visual predictive check (pcVPC) was generated using Pearl-speaks-NONMEM (version 4.7.17; Department of Pharmaceutical Biosciences, Uppsala University Uppsala, Sweden (<https://uupharmacometrics.github.io/PsN/>)) as a model diagnostic tool in addition to diagnostics generated using Xpose (version 4.5.3; Department of Pharmaceutical Biosciences, Uppsala University, Uppsala, Sweden (<http://xpose.sourceforge.net>)). The final model was selected based on the OFV drop at 5% significance level between nested models and the result from pcVPC. R (version 3.3.0; R Foundation for Statistical Computing, Vienna, Austria (<http://www.R-project.org>)) package “ggplot2” and “xpose4” were used to plot and visualize the results. PAE parameter for isoniazid was estimated with “optim” function using Nelder-Mead algorithm in R. All simulations for translational prediction were performed using “deSolve” package in R. The EBA data from Wallis *et al.*²⁰ was digitalized using WebPlotDigitizer (version 4.1; WebPlotDigitizer, Austin, TX (<https://automeris.io/WebPlotDigitizer>)).

RESULTS

The translational MTP-GPDI model approach was developed to predict the EBA of drug combination based on preclinical *in vitro*

study. **Figure 1a** shows the schematic illustration of the translational steps; **Figure 1b** shows the final translational MTP-GPDI model for isoniazid-rifampicin combination with identified PD interactions. Initially, the exposure–response relationship from *in vitro* data using MTP models for isoniazid and rifampicin monotherapy were combined with the GPDI model to evaluate the potential PD interactions of the isoniazid-rifampicin combination. Translational factors, including human PK and the ELF model, bacterial growth phase, PAE, and MIC scaling, were linked to the *in vitro* models to mimic the bacterial growth and drug kinetics in humans. Thereafter, the *in vitro* models and translational factors were applied in clinical trial simulation to predict the EBA. The prediction was then compared with the clinical data from different EBA studies to see the ability of the translational model to predict the clinical observation.

In vitro exposure–response relationships for isoniazid and rifampicin in monotherapy

The NONMEM code of the final model is given in the **Supplementary Material** (NONMEM code). In this study, the MTP model⁵ successfully described and identified the *in vitro* exposure–response relationship of isoniazid at different concentrations using time-kill CFU experiments in log-phase and stationary-phase. The descriptions of the variables in Eqs. 1–6 are available in **Table 1**. Eqs. 1–3 describe the final differential equations system of the MTP model which consists of three different bacterial subpopulations including the number of *F*, *S*, and *N* bacterial substates change over the time as well as isoniazid drug effects.

$$\frac{dF}{dt} = F \cdot k_G \cdot \log \left(\frac{B_{max}}{F+S+N} \right) \cdot EFG + k_{SF} \cdot S - k_{FS} \cdot F - k_{FN} \cdot F - EFD \cdot F \quad (1)$$

$$\frac{dS}{dt} = k_{FS} \cdot F + k_{NS} \cdot N - k_{SN} \cdot S - k_{SF} \cdot S - ESD \cdot S \quad (2)$$

$$\frac{dN}{dt} = k_{SN} \cdot S + k_{FN} \cdot F - k_{NS} \cdot N \quad (3)$$

The isoniazid drug effect was described by a linear inhibition of *F* growth (EFG, Eq. 4) and a power function for the killing of the *F* substate (EFD, Eq. 5). Killing of the *S* substate was described by sigmoid E_{max} function (ESD, Eq. 6). No drug effect was identified on killing of the *N* substate. An inoculum effect²¹ was found to be statistically significant which included a reduction of the killing effect of *F* and *S* bacteria at high bacterial load using a capacity limitation term $\left(1 - \frac{F+S+N}{B_{max}}\right)$ (Eqs. 5 and 6). The drop in OFV was –286.2431 when applied to killing of *F* and *S* bacteria.

$$EFG = 1 - \left(FG_{slope} \cdot C_{INH} \right) \quad (4)$$

$$EFD = FD_{slope} \cdot \left(1 - \frac{F+S+N}{B_{max}} \right) \cdot C_{INH}^{FD_I} \quad (5)$$

$$ESD = \frac{SD_{E_{max}} \cdot \left(1 - \frac{F+S+N}{B_{max}} \right) \cdot C_{INH}^{SD_I}}{SD_{EC50}^{SD_I} + C_{INH}^{SD_I}} \quad (6)$$

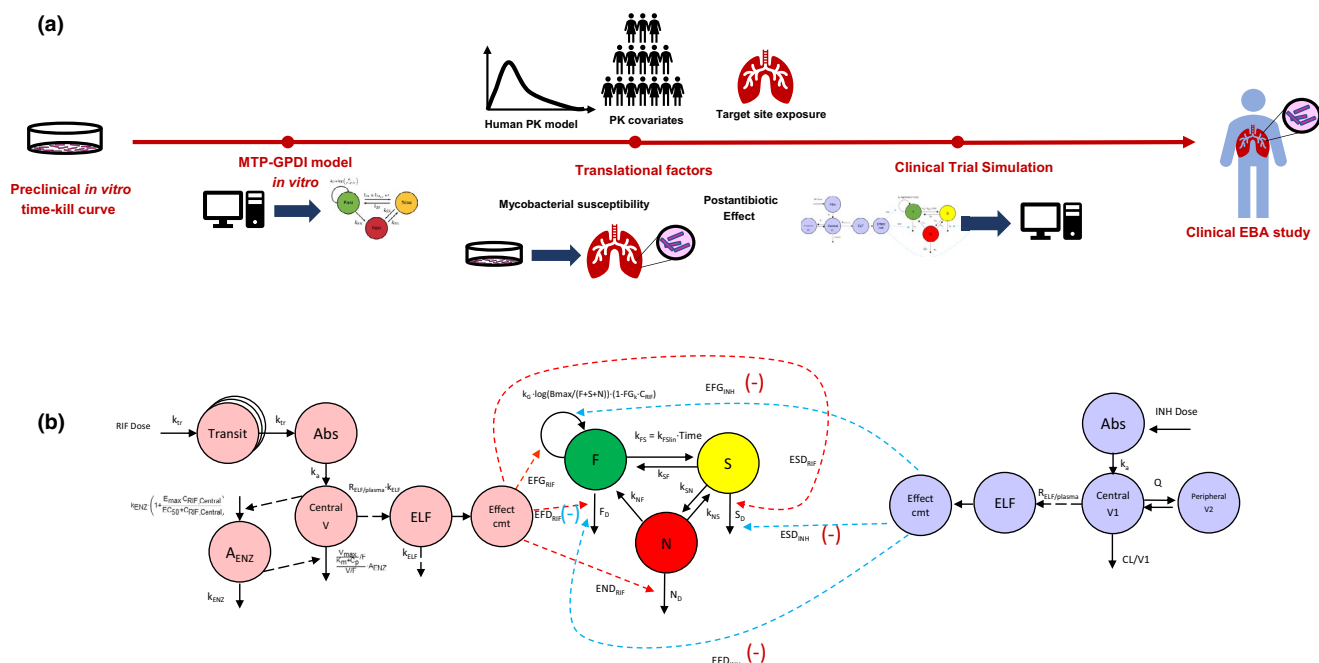


Figure 1 Translational framework for TB (Tuberculosis) drug combination. **(a)** Schematic illustration of translational steps using the MTP-GPDI (Multistate Tuberculosis Pharmacometric-General Pharmacodynamic Interaction) model framework; **(b)** compartmental representation of rifampicin (RIF) pharmacokinetics (PK) (left) and isoniazid (INH) pharmacokinetics (right) linked to pharmacodynamic model (MTP-GPDI model, middle). Enzyme turnover rate stimulated by C_{RIF} (rifampicin concentration) accounting for auto-induction. Solid arrows represent mass flux; dashed arrows represent effects or virtual links. Abs, absorption compartment; A_{ENZ} , enzyme induction compartment; B_{max} , maximum bacterial load; CL, clearance; cmt, compartment; EBA, early bactericidal activity; EFD, drug effect on killing of F bacteria; EFG, drug effect on inhibition of F growth; ELF, epithelial lining fluid; ESD, drug effect on killing of S bacteria; F , fast-multiplying state; F_D , kill rate of F bacteria; k_a , absorption rate; k_{ELF} , ELF transfer rate; k_G , growth rate of the F bacteria; k_{FN} , first-order transfer rate between F and N state; k_{FSLin} , time dependent linear rate parameter describing transfer from F to S state; k_{NS} , first-order transfer rate between N and S state; k_{SF} , first-order transfer rate between S and F state; k_{SN} , first-order transfer rate between S and N state; k_{tr} , transit compartment rate; N , nonmultiplying state; N_D , kill rate of N bacteria; Q , intercompartmental clearance; $R_{ELF/plasma}$, ELF to plasma ratio; S , slow-multiplying state; S_D , kill rate of S bacteria; V , volume of distribution; red minus sign represents the antagonism of rifampicin; red dashed line represents rifampicin drug effect; blue minus sign represents the antagonism of isoniazid; blue dashed line represents isoniazid drug effect.

The final parameter estimates of the MTP model of isoniazid and rifampicin in monotherapy are shown in **Table S1**. In order to avoid the EFG parameter turning into the EFD parameter and the fact that the slope of isoniazid drug effect on the inhibition of F growth (FG_{slope}) was sensitive to different initial estimates, the FG_{slope} was fixed to 0.016. This value represents the slope that gives maximum inhibition of F growth at the highest isoniazid concentration (64 mg/L). Estimating FG_{slope} always gave a value which was higher than 0.016. This is not scientifically plausible and indicates that this parameter turned into EFD. Moreover, fixing this parameter did not significantly change the estimation of other parameters.

The final MTP model for isoniazid in monotherapy was able to capture the log-phase and stationary-phase data as well as the data that were below the LOQ as can be seen in the pcVPC (**Figure 2**). The exposure–response relationship of rifampicin monotherapy *in vitro* using the same strain and experimental setup has been described earlier using the MTP model.⁵

In vitro exposure–response relationships of isoniazid and rifampicin in combination

To assess the PD interaction after identification of the exposure–response relationship in monotherapy, the GPDI model was combined with the MTP model. PD interactions were evaluated as fractional

change of the slope or potency (EC_{50}) in the isoniazid-rifampicin combination. Final parameter estimates for the MTP-GPDI model of isoniazid-rifampicin combination are shown in **Table S1**. The descriptions of the variables in Eqs. 7–16 are available in **Table 1**. Eqs. 7–9 describe how the number of each bacterial state changes over time after exposure to an isoniazid-rifampicin combination. Eqs. 10–16 describe the functions of rifampicin and isoniazid drug effects in combination on inhibition of F growth (EFG_{RIF} , EFG_{INH} ; Eqs. 10 and 11), killing of F state (EFD_{RIF} , EFD_{INH} ; Eqs. 12 and 13), killing of S state (ESD_{RIF} , ESD_{INH} ; Eqs. 14 and 15), and killing of N state (END_{RIF} , Eq. 16) in relation with Eqs. 7–9.

$$\frac{dF}{dt} =$$

$$F \cdot k_G \cdot \log \left(\frac{B_{max}}{F+S+N} \right) \cdot (1 - (EFG_{RIF} + EFG_{INH})) + k_{SF} \cdot S - k_{FS} \cdot F - k_{FN} \cdot F - (EFD_{RIF} + EFD_{INH}) \cdot F \quad (7)$$

$$\frac{dS}{dt} = k_{FS} \cdot F + k_{NS} \cdot N - k_{SN} \cdot S - k_{SF} \cdot S - (ESD_{RIF} + ESD_{INH} - ESD_{RIF} \cdot ESD_{INH}) \cdot S \quad (8)$$

$$\frac{dN}{dt} = k_{SN} \cdot S + k_{FN} \cdot F - k_{NS} \cdot N - END_{RIF} \cdot N \quad (9)$$

Table 1 Parameters of the final MTP-GPDI translational model approach for isoniazid and rifampicin in monotherapy and combination. The model consisted of different submodels such as natural growth, exposure–response relationship of isoniazid and rifampicin monotherapy, PD interaction, PAE model of isoniazid and rifampicin, human PK and ELF model of isoniazid and rifampicin as well as protein binding

Parameter	Description	Value	References
<i>Natural growth</i>			
k_{FN} (days ⁻¹)	Transfer rate from fast-multiplying to nonmultiplying state	8.97×10^{-7}	5
k_{SN} (days ⁻¹)	Transfer rate from slow-multiplying to nonmultiplying state	0.186	5
k_{SF} (days ⁻¹)	Transfer rate from slow-multiplying to fast-multiplying state	0.0145	5
k_{NS} (days ⁻¹)	Transfer rate from nonmultiplying to slow-multiplying state	1.23×10^{-3}	5
$k_{FS,lin}$ (days ⁻²)	Time-dependent transfer rate from fast-multiplying to slow-multiplying state	1.66×10^{-3}	5
S_0 (mL ⁻¹)	Initial bacterial number of slow-multiplying state	9770	5
k_G (days ⁻¹)	Fast-multiplying bacterial growth rate	0.206	5
		0.15 (for PAE model of isoniazid)	Estimated from Chan et al. ¹⁰
F_0 (mL ⁻¹)	Initial bacterial number of fast-multiplying state	4.1	5
B_{max} (mL ⁻¹)	System carrying capacity	1.410×10^9	5
<i>Isoniazid exposure–response relationships monotherapy</i>			
FG_{slope} (L/mg)	Linear inhibition of fast-multiplying bacterial growth	0.016	Table S1
FD_{slope} (L/mg/days)	Slope for power of killing of fast-multiplying bacteria	1.27	Table S1
FD_γ	Power for killing of fast-multiplying bacteria	0.3067	Table S1
SD_{Emax} (days ⁻¹)	Maximal slow-multiplying bacterial kill rate	15.29	Table S1
SD_{EC50} (mg/L)	Isoniazid concentration at which half SD_{Emax} is reached	3.341	Table S1
SD_γ	Hill coefficient of sigmoidicity	1.131	Table S1
<i>Rifampicin exposure–response relationships monotherapy</i>			
FG_{slope} (L/mg)	Linear inhibition of fast-multiplying bacterial growth	0.017	5
FD_{Emax} (days ⁻¹)	Maximal fast-multiplying bacterial kill rate	2.15	5
FD_{EC50} (mg/L)	Rifampicin concentration at which half FD_{Emax} is reached	0.52	5
SD_{Emax} (days ⁻¹)	Maximal slow-multiplying bacterial kill rate	1.56	5
SD_{EC50} (mg/L)	Rifampicin concentration at which half SD_{Emax} is reached	13.4	5
ND_{slope} (L/mg/days)	Linear nonmultiplying kill rate	0.24	5
<i>PD interaction (GPDI model)</i>			
$INT_{RIF,INH}^{FG}$	Interaction of rifampicin to isoniazid on inhibition of <i>F</i> -growth	6.04 (antagonism) ^a	Table S1
$INT_{INH,RIF}^{FD}$	Interaction of isoniazid to rifampicin on killing of <i>F</i> -state	1.828 (antagonism) ^a	Table S1
$INT_{RIF,INH}^{FD}$	Interaction of rifampicin to isoniazid on killing of <i>F</i> -state	1,000 (antagonism) ^a	Table S1
$INT_{RIF,INH}^{SD}$	Interaction of rifampicin to isoniazid on killing of <i>S</i> -state	136.6 (antagonism) ^a	Table S1
<i>PAE model isoniazid</i>			
k_{e0} (day ⁻¹)	Equilibrium rate between ELF and effect compartment of isoniazid	7.5	Estimated from Chan et al. ^{10,11}
<i>PAE model rifampicin</i>			
$k_{e,in}$ (days ⁻¹)	Transfer rate constant into the effect compartment	150	3
$k_{e,out,max}$ (days ⁻¹)	Maximal transfer rate from the effect compartment	1.091	3
$k_{e,out,50}$ (mg/L)	Rifampicin concentration at which half $k_{e,out,max}$ is reached	0.662	3
<i>Isoniazid human PK</i>			
CL_{fast}/F (L/hour)	Apparent clearance for fast acetylators	21.6	15
CL_{slow}/F (L/hour)	Apparent clearance for slow acetylators	9.70	15
V_c/F (L)	Apparent central volume of distribution	57.7	15
V_p/F (L)	Apparent peripheral volume of distribution	1730	15

(Continued)

Table 1 (Continued)

Parameter	Description	Value	References
Q/F (L/hour)	Apparent intercompartmental clearance	3.34	15
k_a (hour ⁻¹)	Absorption rate constant	1.85	15
t_{lag} (hour ⁻¹)	Absorption lag time	0.18	15
P_{fast}	Proportion of fast acetylators in the population	0.132	15
$\theta_{CL,HIV}$	Linear effect of positive HIV status on CL/F	-0.174	15
$\theta_{Vc,sex,F}$	Linear effect of being female on V_c/F	-0.103	15
IIV CL/F (%) ^b	Interindividual variability in CL/F	18.4	15
IIV V_c/F (%) ^b	Interindividual variability in V_c/F	16.5	15
IIV Q/F (%) ^b	Interindividual variability in Q/F	93.1	15
IIV F (%) ^b	Interindividual variability in F	26.2	15
IIV t_{lag} (%) ^b	Interindividual variability in t_{lag}	88.4	15
IOV k_a (%) ^b	Interoccasion variability in k_a	90.1	15
IOV F (%) ^b	Interoccasion variability in F	8.4	15
<i>Isoniazid ELF model</i>			
$R_{ELF/plasma}$ (-) ^c	Epithelial lining fluid/plasma concentration ratio	1.37–5.88	17
<i>Rifampicin human PK and ELF model</i>			
V_{max} (mg/hour/70 kg)	Maximal elimination rate	525	14
k_m (mg/L)	Rifampicin concentration at which half V_{max} is reached	35.3	14
V_d (L/70 kg)	Volume of distribution	87.2	14
k_a (hour ⁻¹)	Absorption rate constant	1.77	14
MTT (hour ⁻¹)	Mean transit time	0.513	14
NN (-)	Number of absorption transit compartments	23.8	14
E_{max} (-)	Maximal increase in enzyme production rate	1.16	14
EC_{50} (mg/L)	Rifampicin concentration at which half the E_{max} is reached	0.0699	14
k_{ENZ} (hour ⁻¹)	First-order rate constant for enzyme pool degradation	6.03×10^{-3}	14
F_{max} (-)	Maximal increase in relative bioavailability at doses above 450 mg	0.504	14
ED_{50} (mg)	Difference in dose above 450 mg at which half the F_{max} is reached	67.0	14
IIV V_{max} (%) ^b	Interindividual variability in V_{max}	30.0	14
IIV k_m (%) ^b	Interindividual variability in k_m	35.8	14
IIV V_d (%) ^b	Interindividual variability in V_d	7.86	14
IIV k_a (%) ^b	Interindividual variability in k_a	33.8	14
IIV MTT (%) ^b	Interindividual variability in MTT	38.2	14
IIV NN (%) ^b	Interindividual variability in NN	77.9	14
IOV k_m (%) ^b	Interoccasion variability in k_m	18.9	14
IOV k_a (%) ^b	Interoccasion variability in k_a	31.4	14
IOV MTT (%) ^b	Interoccasion variability in MTT	56.4	14
IOV F (%) ^b	Interoccasion variability in F	15.7	14
Correlation $V_{max}-k_m$ (%)		38.9	14
<i>Rifampicin ELF model</i>			
k_{ELF} (hour ⁻¹)	Transfer rate constant from plasma to epithelial lining fluid	41.58	18
$R_{ELF/plasma}$ (-)	Epithelial lining fluid/plasma concentration ratio	0.26	18
<i>Protein binding</i>			
$f_{u,rif}$ (-)	Fraction unbound of rifampicin	0.2	18
$f_{u,inh}$ (-)	Fraction unbound of isoniazid	0.9	16

PAE, postantibiotic effect.

^aAntagonism represents the effect less than expected additivity in biomarker level. ^bIIV and IOV parameters are expressed as coefficient of variation and as a percentage of the parameter estimate. ^cDuring the simulation, random numbers were generated from uniform distribution using the minimum value of 1.37 and the maximum value of 5.88.

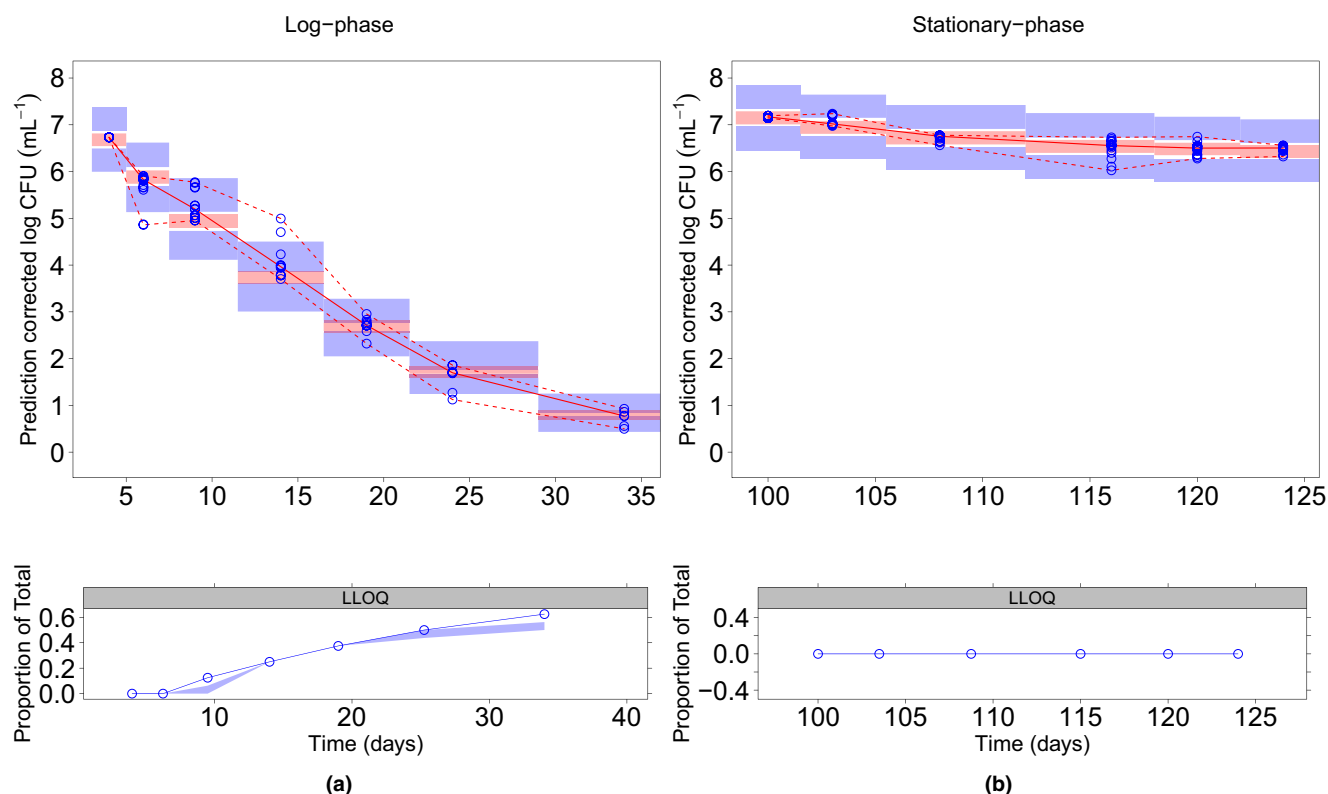


Figure 2 The pcVPC (prediction-corrected visual predictive check) for the final MTP (Multistate Tuberculosis Pharmacometric) model and isoniazid in monotherapy applied to *in vitro* (a) log-phase data and (b) stationary-phase data. Open blue circles represent prediction-corrected observed \log_{10} CFU (colony-forming unit) data after different isoniazid concentrations at constant exposure (0.25–64 mg/L); red solid line shows the median of observed data; red dashed lines are the 5th and 95th percentiles of the observed data. Top and bottom blue shaded areas are the 95% confidence intervals (CIs) for the 5th and 95th percentiles of simulated data; the middle red shaded areas are the 95% CI for the median of simulated data. The blue solid line in the lower panel is the median of the data below the LOQ (limit of quantification). The blue shaded area in the lower panel is the 95% CI for the simulated LOQ data. LLOQ, lower than limit of quantification.

$$EFG_{RIF} = \frac{FG_{slope}^{RIF}}{\left(1 + \frac{INT_{INH,RIF}^{FG} \cdot C_{INH}}{0.00001 + C_{INH}}\right)} \cdot C_{RIF} \quad (10)$$

$$EFG_{INH} = \frac{FG_{slope}^{INH}}{\left(1 + \frac{INT_{RIF,INH}^{FG} \cdot C_{RIF}}{0.00001 + C_{RIF}}\right)} \cdot C_{INH} \quad (11)$$

$$EFD_{RIF} = \frac{FD_{Emax}^{RIF} \cdot C_{RIF}}{\left(FD_{EC50}^{RIF} \cdot \left(1 + \frac{INT_{INH,RIF}^{FD} \cdot C_{INH}}{0.00001 + C_{INH}}\right)\right) + C_{RIF}} \quad (12)$$

$$EFD_{INH} = \frac{FD_{slope}^{INH}}{\left(1 + \frac{INT_{RIF,INH}^{FD} \cdot C_{RIF}}{FD_{EC50}^{RIF} + C_{RIF}}\right)} \cdot \left(1 - \frac{F+S+N}{B_{max}}\right) \cdot C_{INH}^{FD\gamma} \quad (13)$$

$$ESD_{RIF} = \frac{\frac{SD_{Emax}^{RIF}}{SD_{Emax}^{INH}} \cdot C_{RIF}}{\left(SD_{EC50}^{RIF} \cdot \left(1 + \frac{INT_{INH,RIF}^{SD} \cdot C_{INH}}{0.00001 + C_{INH}}\right)\right) + C_{RIF}} \quad (14)$$

$$ESD_{INH} = \frac{1 \cdot \left(1 - \frac{F+S+N}{B_{max}}\right) \cdot C_{INH}^{SD\gamma}}{\left(\left(SD_{EC50}^{INH} \cdot \left(1 + \frac{INT_{RIF,INH}^{FD} \cdot C_{RIF}}{FD_{EC50}^{RIF} + C_{RIF}}\right)\right)^{SD\gamma}\right) + C_{INH}^{SD\gamma}} \quad (15)$$

$$END_{RIF} = ND_{slope}^{RIF} \cdot C_{RIF} \quad (16)$$

According to this study, bidirectional antagonism was identified where rifampicin and isoniazid antagonized one another. Rifampicin became a perpetrator towards the isoniazid effect on *F* growth, killing of *F* and *S* states. The maximum fractional change of the slope of isoniazid in the presence of rifampicin in the killing of *F* state ($INT_{RIF,INH}^{FD}$) parameter was fixed at 1,000 because NONMEM estimated it at a very high value (indicating a strong antagonism on this rate constant) with a high parameter uncertainty. Fixing it at 1,000 did not significantly change the model fit ($\Delta OFV = 0.0629$) and the parameter estimates of other parameters. Furthermore, isoniazid acted as a perpetrator towards rifampicin only on the killing of *F* state. There was no interaction identified on killing of *N* state. Due to the fact that EC_{50} of the interaction parameter was difficult to estimate, some of the EC_{50} of the interactions were set at a very low value 1×10^{-5} (Eq. 10, 11, 12, 14) leading to an on/off interaction.

The final MTP-GPDI model well described the isoniazid-rifampicin data at different concentrations in the stationary-phase data. The pcVPC also showed that the model can capture the mean and percentiles of the observations relatively well (**Figure 3**). The M3 method was also able to handle the data below LOQ, although there was an underprediction at 110 days.

Clinical phase IIa EBA predictions

All parameter values for translational prediction are listed in **Table 1**, and the illustration of the final translational MTP-GPDI model for isoniazid-rifampicin combination is shown in **Figure 1b**.

The translational MTP model for isoniazid monotherapy successfully predicted the dose–response relationship of EBA_{0–2 days}, EBA_{0–5 days}, and EBA_{0–14 days}. The prediction could also capture the EBA observation from different studies^{1,22–25} at a wide range of isoniazid doses in the mixed population of fast and slow acetylators (**Figure 4**). During the estimation of the PAE parameter for isoniazid, the growth rate of fast-multiplying bacteria was estimated to be 0.15 in order to mimic the growth control curve from

Chan *et al.*¹⁰ The inoculum effect was removed during the translational prediction because this phenomenon occurs due to the restrictions in bacterial nutrients and space *in vitro* which may not apply in the lung. Our result also supported this argument because the EBA prediction was very low when the inoculum effect term was included (**Figure S3a**).

When the *in vitro* MIC distribution¹² in *M. tuberculosis* H37Rv was included in the prediction (**Figure S3b**), more EBA observations were captured by the model prediction. However, this implied that we included more variability of MIC measurement in the prediction. Using the mode of the *in vitro* MIC distribution (0.06 mg/L) was preferred because it still gave a good prediction and captured most of the EBA observations. The simulation also showed that maximal efficacy has been reached for isoniazid in mixed populations of slow and fast acetylators (**Figure 4**). Increasing the dose above 300 mg of isoniazid did not contribute significantly to a higher EBA specifically on EBA_{0–14 days}.

The EBA predictions of isoniazid in monotherapy were also done for distinctly different groups with respect to acetylator status, i.e., for fast and slow acetylators. The slow acetylator population (**Figure S4a**) showed a relatively higher EBA at all dose levels compared with the fast acetylator population (**Figure S4b**). However, increasing the dose from 300 mg to 900 mg for both fast and slow acetylators did not substantially increase the EBA, especially at day 14.

The clinical prediction of rifampicin monotherapy has been shown in an earlier study³ and was incorporated into the simulation of the isoniazid-rifampicin combinations in this study. The translational MTP-GPDI model for isoniazid-rifampicin combination also successfully predicted the dose–response relationship of EBA_{0–2 days} and EBA_{0–14 days}. Although the EBA observations^{1,20} for the combination were very limited, the model was able to predict the observations well (**Figure 5**). We believe that one of the two trials providing EBA_{0–2 days} data had an extreme outcome indicated by a very high efficacy, i.e., very high EBA_{0–2 days}, and as such cannot be captured by the 95% prediction interval of the translational framework (**Figure 5**). The checkerboard plot of rifampicin and isoniazid at different doses (**Figure 6**) also indicated that increasing the rifampicin dose results in higher efficacy, although increasing the isoniazid dose will not significantly improve the EBA of the combination. The reason for this is due to the antagonism of isoniazid-rifampicin combination identified from exposure–response relationship from the *in vitro* data. The *in vitro* data showed that increasing rifampicin concentration in combination can increase the bacterial killing (**Figure S2a**). On the other hand, increasing isoniazid concentration in combination did not significantly increase the bacterial killing (**Figure S2b**).

Sensitivity analysis

In order to analyze how each translational factor affected the prediction of clinical data of isoniazid in monotherapy, a sensitivity analysis was performed by removing one translational factor at a time from the final translational model. Removing PAE from the model did not affect the prediction (**Figure S5a** vs. **Figure 4**). Exclusion of MIC scaling also did not considerably

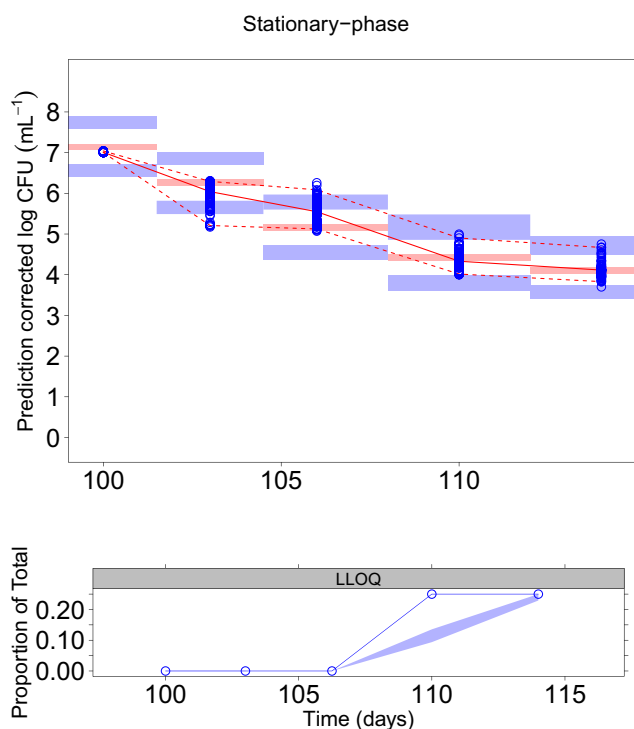


Figure 3 The pcVPC (prediction-corrected visual predictive check) for the final MTP-GPDI (Multistate Tuberculosis Pharmacometric-General Pharmacodynamic Interaction) model and *in vitro* stationary-phase data of isoniazid-rifampicin in combination. Open blue circles represent prediction-corrected observed log₁₀ CFU data after different concentrations at constant exposure (rifampicin 0.5–64 mg/L and isoniazid 2–64 mg/L); solid red line shows the median of observed data; red dash lines are the 5th and 95th percentiles of the observed data. Top and bottom blue shaded areas are the 95% CIs for the 5th and 95th percentiles of simulated data, and the middle red shaded areas are the 95% CI for the median of simulated data. The blue solid line in the lower panel is the median of the data below the LOQ (limit of quantification). The blue shaded area in the lower panel is the 95% CI for the simulated LOQ data. LLOQ, lower than limit of quantification.

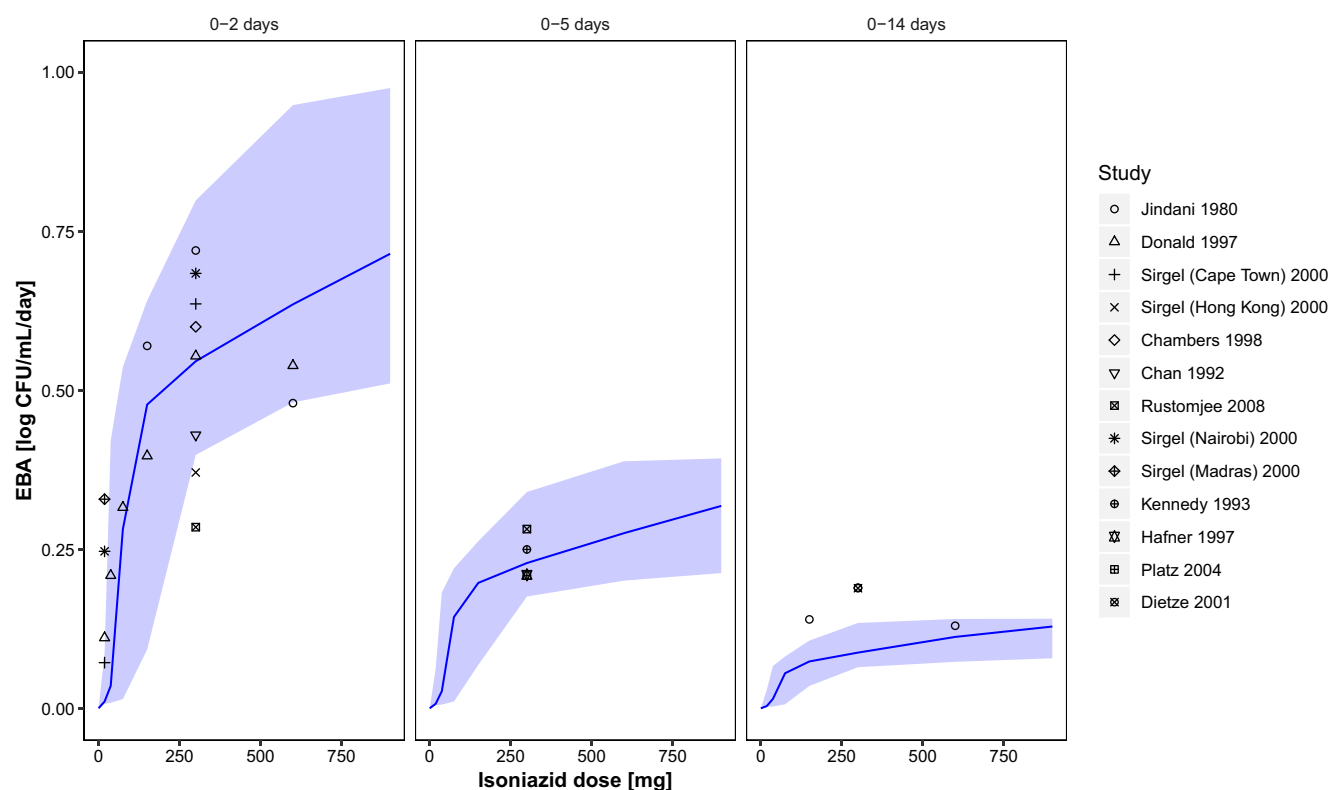


Figure 4 Clinical prediction ($EBA_{0-2\text{ days}}$, $EBA_{0-5\text{ days}}$, and $EBA_{0-14\text{ days}}$) of the final translational MTP (Multistate Tuberculosis Pharmacometric) model for isoniazid monotherapy at different doses of isoniazid in mixed populations of fast acetylators (13.2%) and slow acetylators (86.8%). Blue solid line is the median of the prediction; blue shaded area represents the 5th to 95th percentile of the prediction; points with different shapes represent the clinical observations from different studies. EBA, early bactericidal activity.

influence the prediction (**Figure S5b** vs. **Figure 4**). On the other hand, changing the preincubation period from 150 days to 4 days affected the prediction significantly (**Figure S5c** vs. **Figure 4**). An earlier publication investigated a sensitivity analysis for rifampicin in monotherapy in a similar way and found that exclusion of PAE, MIC scaling, and changing preincubation period substantially affected the EBA prediction.³ For the final translational model of isoniazid-rifampicin combination, sensitivity analysis was done by excluding each INT parameter which represents maximum fractional change of the victim's drug effect parameter caused by perpetrator. Exclusion of $INT_{RIF,INH}^{FD}$, $INT_{INH,RIF}^{FD}$, and $INT_{RIF,INH}^{FG}$ (**Figure S6a-c**) did not considerably influence the prediction, but exclusion of $INT_{RIF,INH}^{SD}$ shifted the EBA to a relatively high value (**Figure S6d**).

DISCUSSION

The EBA study in phase IIa trials is commonly performed to demonstrate bactericidal activity of a drug in monotherapy in early treatment. In this study, we aimed to develop an approach to streamline the translation of preclinical *in vitro* information into dose suggestions for clinical phase IIa EBA trials evaluating antituberculosis drug combinations. The translational MTP-GPDI model approach that we have developed for isoniazid and rifampicin in monotherapy and combination in this work successfully predicted the drug effect from different EBA studies using *in vitro*

information. This could help in the design of early TB combination trials accounting for PD interaction of the drug combination.

The MTP model was originally derived using *in vitro* natural growth data spanning up to 200 days. After ~ 100 days, the bacteria are going into the stationary-phase which was seen as a decrease in CFU.⁵ This informed the model about the rate of transfer from the *S* state to the *N* state. In further exposure-response analysis, these rates are fixed, and the drug effect can then be quantified for all three states. The advantage of this approach compared with simpler models is that the MTP model can describe the dynamics of different mycobacterial states (*F*, *S*, and *N*) using CFU data, although CFU only accounted for the number of actively growing bacteria. This can identify drug effect for drugs with a majority of drug efficacy on *N* state even in EBA phase IIa study, such as for clofazimine,²⁶ for which a simpler analysis would have concluded that the drug had no efficacy based on phase IIa data.

Among other TB drugs, isoniazid is known for its high early bactericidal activity. According to the MTP model *in vitro*, isoniazid exhibited the effect towards inhibition of growth of *F*, killing of *F*, and killing of *S* state bacteria. This result was consistent with the literature that isoniazid as a cell wall inhibitor kills only actively growing bacteria but displays very limited sterilizing activity against persisters.^{27,28} There was no trend in the observed data that there was emergence of resistance during the experimental study time, although this has been shown for other experiments *in*

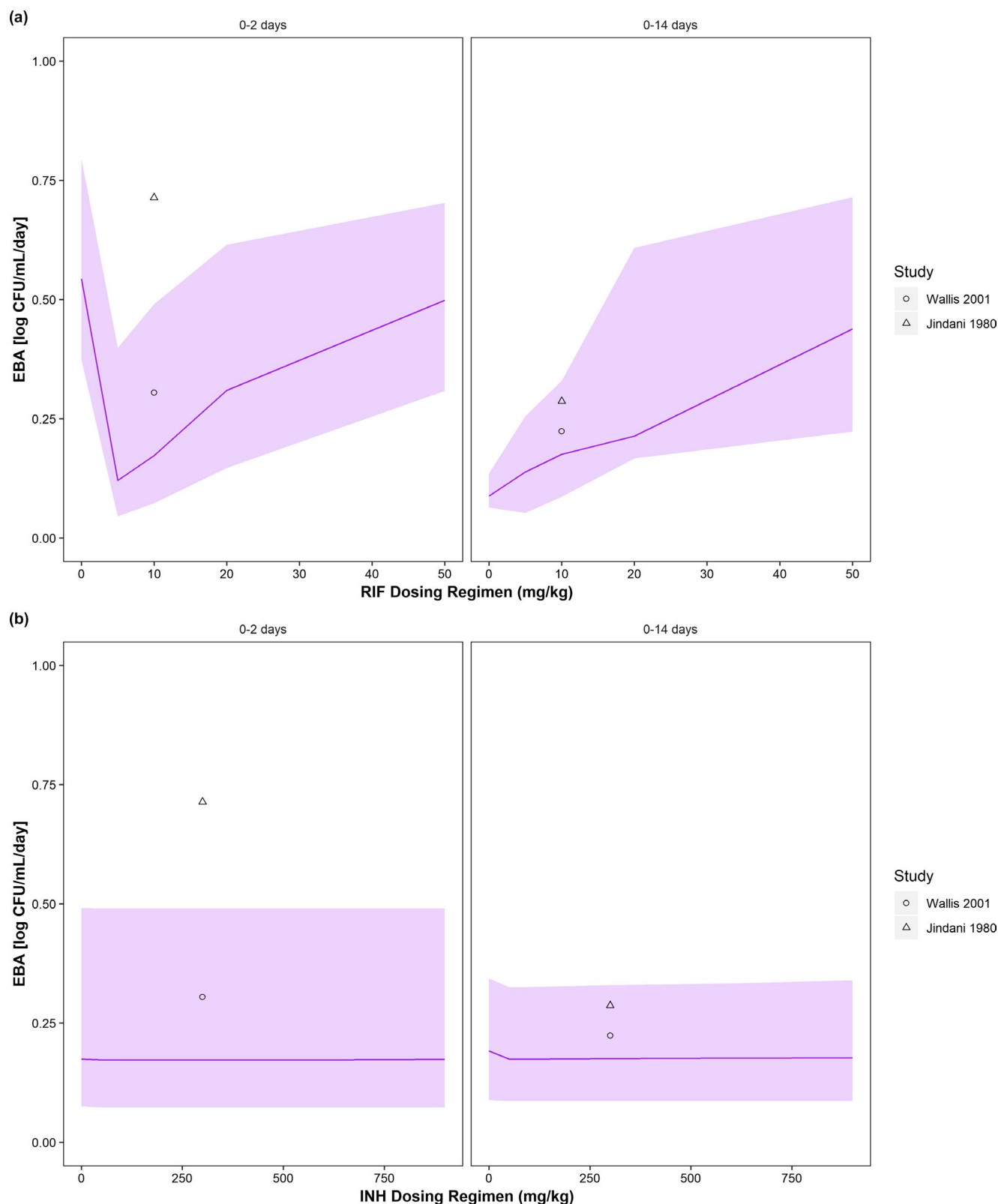


Figure 5 Clinical prediction ($EBA_{0-2 \text{ days}}$ and $EBA_{0-14 \text{ days}}$) of the final translational MTP-GPDI (Multistate Tuberculosis Pharmacometric-General Pharmacodynamic Interaction) model for isoniazid-rifampicin combination in mixed populations of fast acetylators (13.2%) and slow acetylators (86.8%). **(a)** 300 mg isoniazid combined with different doses of rifampicin. **(b)** 10 mg/kg rifampicin combined with different doses of isoniazid. Solid purple line is the median of the prediction; shaded purple area represents the 5th to 95th percentile of the prediction; points with different shapes represent the clinical observations from different studies. CFU, colony-forming unit; EBA, early bactericidal activity; INH, isoniazid; RIF, rifampicin.

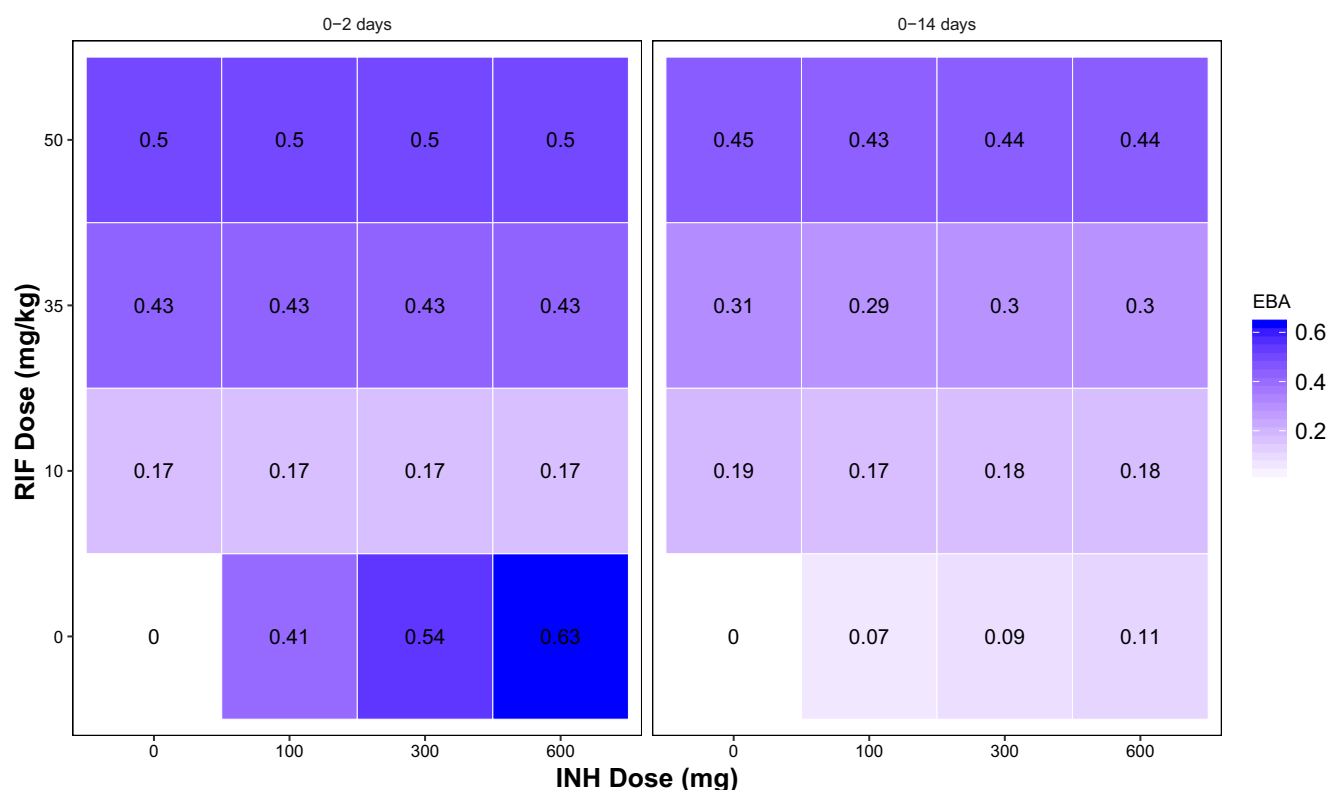


Figure 6 The checkerboard plot of $EBA_{0-2 \text{ days}}$ and $EBA_{0-14 \text{ days}}$ at different isoniazid-rifampicin dose combinations. The color was based on the EBA (log CFU/mL/day) value of each regimen, where white indicated the low EBA, purple indicated medium EBA, and blue indicated the high EBA. CFU, colony-forming unit; EBA, early bactericidal activity; INH, isoniazid; RIF, rifampicin.

vitro.⁶ It is believed that isoniazid resistance development cannot occur during treatment within an individual.²⁹

The translational prediction of isoniazid monotherapy showed that isoniazid had the highest activity at $EBA_{0-2 \text{ days}}$ compared with $EBA_{0-5 \text{ days}}$ and $EBA_{0-14 \text{ days}}$, which indicates high bactericidal activity but low sterilizing activity.¹ The model predictions showed a higher agreement with the observed data for the $EBA_{0-2 \text{ days}}$ and $EBA_{0-5 \text{ days}}$ compared with the $EBA_{0-14 \text{ days}}$ (Figure 4). However, there was limited observed clinical data for the $EBA_{0-14 \text{ days}}$ predictions, simply because of ethical reasons of giving monotherapy for 14 days and risk for resistance development. As such there were only three mean observations from clinical trials compared with 18 mean observations of clinical studies contributing with observed data for the shorter time periods. For this longer $EBA_{0-14 \text{ days}}$ time period, two of the mean observed data points were outside the 95% prediction interval as given by the translational framework. The 95% prediction interval in our simulation means that there is still a 5% possibility that the observation lies outside the prediction interval and, as such, some of the observed data (5%) should lie outside the prediction interval.

Because higher doses of isoniazid have not been studied as extensively as rifampicin, we only had limited data for the higher dose of isoniazid. However, we can still predict lower and standard isoniazid doses using our approach in order to inform future clinical trials. The prediction of higher dose was also in agreement with the study from Donald *et al.*, where the maximum effect of isoniazid was reached at a dose 300 mg, which indicated that increasing the isoniazid dose did not increase the efficacy.²²

Due to the extensive metabolism of isoniazid in the fast acetylator population, several studies have shown lower isoniazid exposure in the fast acetylator than the slow acetylator population.^{30,31} Similar to our results (Figure S4), the EBA study from Donald *et al.* also demonstrated that the EBA of the fast acetylator group was lower compared with the slow acetylator group.³² However, other studies have shown that low isoniazid exposure had no significant correlation with the efficacy.^{31,33,34} They demonstrated that the standard dose is enough for both acetylator groups and the higher dose for the fast acetylator population is only relevant for once weekly regimens.^{31-33,35}

In the current study, rifampicin showed inhibition towards the isoniazid effect on the growth of *F*, killing of *F* state, and killing of *S* state, but isoniazid only inhibited the rifampicin effect on killing of *S* based on the *in vitro* MTP-GPDI model. This is also in line with earlier findings from Chen *et al.* in a mouse study using the MTP-GPDI model in which the activity of the combination of rifampicin and isoniazid was predicted to be lower than the expected additivity.⁷ However, in another mouse study it was shown that the isoniazid and rifampicin combination interacted additively,³⁶ but it was not clear how the interaction effect compared with the expected additivity on the biomarker level. When comparing the interaction in stationary-phase data in our study with the interaction in the log-phase data from Clewe *et al.*,⁶ rifampicin had a synergistic effect on isoniazid killing *F* state bacteria, which indicated that the interaction can differ in different growth phase.

The translational prediction of combination therapy showed an interesting “V shape” curve (**Figure 5a**), which originates from the antagonistic interaction. According to the study from Rockwood *et al.*, isoniazid showed concentration-dependent antagonism on 2-month culture conversion when isoniazid maximum concentration (C_{\max}) was < 4.6 mg/L and rifampicin C_{\max} /MIC was < 28.³⁷ In this situation, increasing rifampicin C_{\max} /MIC can counteract the antagonistic effect of isoniazid.³⁷

The clinical prediction of this study indicated that increasing the dose of isoniazid in combination therapy will not increase the EBA, regardless of acetylator status. Although there is no clinical study comparing different doses of isoniazid-rifampicin in combination, the work confirms clinical trials showing an increased efficacy of rifampicin at higher doses and no benefit of increasing the isoniazid dose.^{22,38} However, these results need to be interpreted with caution since they were only predictions for short-term efficacy where there is still an unclear relationship with long-term efficacy. More studies are needed to predict the long-term efficacy using this approach in order to optimize the dose for current TB treatment as well as for new TB drugs in clinical drug development. The optimal dose of the combination also needs to take into account safety and tolerability of the two drugs in combination.

The limitation in our study is that there were not enough data available in the literature to estimate the PAE parameter for isoniazid-rifampicin combination. The study was also limited by the lack of EBA data in the literature for isoniazid-rifampicin combination, which made it difficult to see how good our translational model performs to capture the EBA for different dose combinations in isoniazid-rifampicin combination. In our work, we used static and not dynamic *in vitro* data to characterize the exposure–response relationship. A study from Nielsen *et al.* has shown that a pharmacokinetics–pharmacodynamics (PKPD) model with parameter estimates based on data from only the static time-kill curve experiments in *Streptococcus pyogenes* could predict the majority of the time-kill curves data from the dynamic experiments reasonably well.³⁹ Although for some drugs, differences in sensitivity to experimental conditions were noted.³⁹

Drug exposure in the lesion may be the true site of action, especially for persistent bacteria. However, all drugs need to be unbound in order to pass through membrane irrespectively of site of action. The concentrations in the ELF were unbound concentrations and should reflect target site concentrations where the plasma/tissue ratio is the same for ELF. For caseous lesions, the ratio to plasma might be lower due to permeability issues. More work is needed in order to understand these distribution processes. Future drug distribution models for caseous lesions could be incorporated into this translational framework. In our work we included an effect compartment in our translational model to account for an effect delay. In this case, the delay might include the transfer of the drug from the ELF to lesions.

In order to identify a precise exposure–response relationship using *in vitro* experiments, the *in vitro* designs need to incorporate drug exposure in wide range, not only the most likely clinical exposure. Similarly, in order to define PD interactions using *in vitro* information, experimental designs need to cover a wide range of exposure levels for the drugs of interest, not only one exposure level of each drug. Optimal experimental designs for *in vitro* experiments for identification of PD

interactions have been studied, and a rational design using only information about the EC_{50} of each drug from monotherapy is used to inform the design of the PD interaction studies.⁸

It is important that EBA studies are designed and analyzed in such a manner that an efficient clinical trial study is designed and analyzed with high power. Earlier work has shown that a PKPD model approach using the same underlying disease model as in this work, i.e., the MTP model, had twofold higher power for EBA studies compared with traditional studies.⁴⁰ Further, a PKPD model approach for liquid EBA studies has been shown to have a higher power since a traditional analysis did not reveal a statistically significant exposure–response relationship for higher doses of rifampicin, whereas a statistically significant exposure–response relationship using the same data was identified in a PKPD model-based analysis.³⁸

In conclusion, our translational approach using the MTP-GPDI model from *in vitro* experiments coupled with translational factors can be used to guide dose selection in phase IIa EBA trials for TB combination therapy. This approach can possibly support testing more combination treatment regimens in phase IIa EBA trials in order to accelerate TB drug development.

SUPPORTING INFORMATION

Supplementary information accompanies this paper on the *Clinical Pharmacology & Therapeutics* website (www.cpt-journal.com).

Figure S1.
Figure S2.
Figure S3.
Figure S4.
Figure S5.
Figure S6.
Table S1.
NONMEM Code.

FUNDING

The Swedish Research Council (grant number 521-2011-3442) and the Innovative Medicines Initiative Joint Undertaking (www.imi.europe.eu) under grant agreement no. 115337, resources of which are composed of financial contribution from the European Union's Seventh Framework Programme (FP7/2007-2013) and EFPIA companies' in-kind contributions.

CONFLICT OF INTEREST

The authors declared no competing interests for this work.

AUTHOR CONTRIBUTIONS

All authors wrote the manuscript, designed the research, performed the research, and analyzed the data.

© 2020 The Authors. *Clinical Pharmacology & Therapeutics* published by Wiley Periodicals, Inc. on behalf of American Society for Clinical Pharmacology and Therapeutics.

This is an open access article under the terms of the Creative Commons Attribution-NonCommercial License, which permits use, distribution and reproduction in any medium, provided the original work is properly cited and is not used for commercial purposes.

1. Jindani, A., Aber, V.R., Edwards, E.A. & Mitchison, D.A. The early bactericidal activity of drugs in patients with pulmonary tuberculosis. *Am. Rev. Respir. Dis.* **121**, 939–949 (1980).
2. Diacon, A.H. *et al.* 14-day bactericidal activity of PA-824, bedaquiline, pyrazinamide, and moxifloxacin combinations: a randomised trial. *Lancet* **380**, 986–993 (2012).

3. Wicha, S.G. *et al.* Forecasting clinical dose–response from preclinical studies in tuberculosis research: translational predictions with rifampicin. *Clin. Pharmacol. Ther.* **104**, 1208–1218 (2018).
4. Wicha, S.G., Chen, C., Clewe, O. & Simonsson, U.S.H. A general pharmacodynamic interaction model identifies perpetrators and victims in drug interactions. *Nat. Commun.* **8**, 2129 (2017).
5. Clewe, O., Aulin, L., Hu, Y., Coates, A.R.M. & Simonsson, U.S.H. A multistate tuberculosis pharmacometric model: a framework for studying anti-tubercular drug effects *in vitro*. *J. Antimicrob. Chemother.* **71**, 964–974 (2016).
6. Clewe, O., Wicha, S.G., de Vogel, C.P., de Steenwinkel, J.E.M. & Simonsson, U.S.H. A model-informed preclinical approach for prediction of clinical pharmacodynamic interactions of anti-TB drug combinations. *J. Antimicrob. Chemother.* **73**, 437–447 (2018).
7. Chen, C. *et al.* Assessing pharmacodynamic interactions in mice using the multistate tuberculosis pharmacometric and general pharmacodynamic interaction models. *CPT Pharmacometrics Syst. Pharmacol.* **6**, 787–797 (2017).
8. Chen, C., Wicha, S.G., Nordgren, R. & Simonsson, U.S.H. Comparisons of analysis methods for assessment of pharmacodynamic interactions including design recommendations. *AAPS J.* **20**, 77 (2018).
9. Mackenzie, F.M. & Gould, I.M. The post-antibiotic effect. *J. Antimicrob. Chemother.* **32**, 519–537 (1993).
10. Chan, C.-Y., Au-Yeang, C., Yew, W.-W., Leung, C.-C. & Cheng, A.F.B. *In vitro* postantibiotic effects of rifapentine, isoniazid, and moxifloxacin against *Mycobacterium tuberculosis*. *Antimicrob. Agents Chemother.* **48**, 340–343 (2004).
11. Chan, C.Y., Au-Yeang, C., Yew, W.W., Hui, M. & Cheng, A.F.B. Postantibiotic effects of antituberculosis agents alone and in combination. *Antimicrob. Agents Chemother.* **45**, 3631–3634 (2001).
12. Kaniga, K. *et al.* A multilaboratory, multicountry study to determine MIC quality control ranges for phenotypic drug susceptibility testing of selected first-line antituberculosis drugs, second-line injectables, fluoroquinolones, clofazimine, and linezolid. *J. Clin. Microbiol.* **54**, 2963–2968 (2016).
13. Schön, T. *et al.* Evaluation of wild-type MIC distributions as a tool for determination of clinical breakpoints for *Mycobacterium tuberculosis*. *J. Antimicrob. Chemother.* **64**, 786–793 (2009).
14. Svensson, R.J. *et al.* A population pharmacokinetic model incorporating saturable pharmacokinetics and autoinduction for high rifampicin doses. *Clin. Pharmacol. Ther.* **103**, 674–683 (2018).
15. Wilkins, J.J. *et al.* Variability in the population pharmacokinetics of isoniazid in South African tuberculosis patients. *Br. J. Clin. Pharmacol.* **72**, 51–62 (2011).
16. Herrera, A.M., Scott, D.O. & Lunte, C.E. Microdialysis sampling for determination of plasma protein binding of drugs. *Pharm. Res.* **7**, 1077–1081 (1990).
17. Conte Jr, J.E. *et al.* Effects of gender, AIDS, and acetylase status on intrapulmonary concentrations of isoniazid. *Antimicrob. Agents Chemother.* **46**, 2358–2364 (2002).
18. Clewe, O., Goutelle, S., Conte Jr, J.E. & Simonsson, U.S.H. A pharmacometric pulmonary model predicting the extent and rate of distribution from plasma to epithelial lining fluid and alveolar cells - using rifampicin as an example. *Eur. J. Clin. Pharmacol.* **71**, 313–319 (2015).
19. Beal, S.L. Ways to fit a PK model with some data below the quantification limit. *J. Pharmacokinet. Pharmacodyn.* **28**, 481–504 (2001).
20. Wallis, R.S. *et al.* Inhibition of isoniazid-induced expression of *Mycobacterium tuberculosis* antigen 85 in sputum: potential surrogate marker in tuberculosis chemotherapy trials. *Antimicrob. Agents Chemother.* **45**, 1302–1304 (2001).
21. Nielsen, E.I. & Friberg, L.E. Pharmacokinetic-pharmacodynamic modeling of antibacterial drugs. *Pharmacol. Rev.* **65**, 1053–1090 (2013).
22. Donald, P.R. *et al.* The early bactericidal activity of isoniazid related to its dose size in pulmonary tuberculosis. *Am. J. Respir. Crit. Care Med.* **156**, 895–900 (1997).
23. Sirgel, F.A. *et al.* A multicentre study of the early bactericidal activity of anti-tuberculosis drugs. *J. Antimicrob. Chemother.* **45**, 859–870 (2000).
24. Rustonjee, R. *et al.* Early bactericidal activity and pharmacokinetics of the diarylquinoline TMC207 in treatment of pulmonary tuberculosis. *Antimicrob. Agents Chemother.* **52**, 2831–2835 (2008).
25. Donald, P.R. & Diacon, A.H. The early bactericidal activity of anti-tuberculosis drugs: a literature review. *Tuberculosis (Edinb.)* **88**, S75–S83 (2008).
26. Faraj, A., Svensson, R.J., Diacon, A.H. & Simonsson, U.S.H. Drug effect of clofazimine on persisting mycobacteria explain an unexpected increase in bacterial load from patients. Poster presented at: Population Approach Group Europe (PAGE) twenty-eighth meeting, Stockholm, Sweden, June 11–14, 2019 <www.page-meeting.org/?abstract=8823>. Abstract 8823.
27. Mitchison, D.A. & Coates, A.R.M. Predictive *in vitro* models of the sterilizing activity of anti-tuberculosis drugs. *Curr. Pharm. Des.* **10**, 3285–3295 (2004).
28. Herbert, D., Paramasivan, C.N., Venkatesan, P., Kubendiran, G., Prabhakar, R. & Mitchison, D.A. Bactericidal action of ofloxacin, sulbactam-ampicillin, rifampin, and isoniazid on logarithmic- and stationary-phase cultures of *Mycobacterium tuberculosis*. *Antimicrob. Agents Chemother.* **40**, 2296–2299 (1996).
29. Mitchison, D.A., Jindani, A., Davies, G.R. & Sirgel, F. Isoniazid activity is terminated by bacterial persistence. *J. Infect. Dis.* **195**, 1871–1872 (2007).
30. Zabost, A. *et al.* Correlation of N-acetyltransferase 2 genotype with isoniazid acetylation in Polish tuberculosis patients. *Biomed Res. Int.* **2013**, 853602 (2013).
31. Burhan, E. *et al.* Isoniazid, rifampin, and pyrazinamide plasma concentrations in relation to treatment response in Indonesian pulmonary tuberculosis patients. *Antimicrob. Agents Chemother.* **57**, 3614–3619 (2013).
32. Donald, P.R. *et al.* The Influence of human N-acetyltransferase genotype on the early bactericidal activity of isoniazid. *Clin. Infect. Dis.* **39**, 1425–1430 (2004).
33. Donald, P.R. *et al.* The influence of dose and N -acetyltransferase-2 (NAT2) genotype and phenotype on the pharmacokinetics and pharmacodynamics of isoniazid. *Eur. J. Clin. Pharmacol.* **63**, 633–639 (2007).
34. Park, J.S. *et al.* Serum levels of antituberculosis drugs and their effect on tuberculosis treatment outcome. *Antimicrob. Agents Chemother.* **60**, 92–98 (2016).
35. Ellard, G.A. Variations between individuals and populations in the acetylation of isoniazid and its significance for the treatment of pulmonary tuberculosis. *Clin. Pharmacol. Ther.* **19**, 610–625 (1976).
36. Almeida, D. *et al.* Paradoxical effect of isoniazid on the activity of rifampin-pyrazinamide combination in a mouse model of tuberculosis. *Antimicrob. Agents Chemother.* **53**, 4178–4184 (2009).
37. Rockwood, N. *et al.* Concentration-dependent antagonism and culture conversion in pulmonary tuberculosis. *Clin. Infect. Dis.* **64**, 1350–1359 (2017).
38. Svensson, R.J. *et al.* Greater early bactericidal activity at higher rifampicin doses revealed by modeling and clinical trial simulations. *J. Infect. Dis.* **218**, 991–999 (2018).
39. Nielsen, E.I., Cars, O. & Friberg, L.E. Predicting *in vitro* antibacterial efficacy across experimental designs with a semimechanistic pharmacokinetic-pharmacodynamic model. *Antimicrob. Agents Chemother.* **55**, 1571–1579 (2011).
40. Svensson, R.J., Gillespie, S.H. & Simonsson, U.S.H. Improved power for TB Phase IIa trials using a model-based pharmacokinetic – pharmacodynamic approach compared with commonly used analysis methods. *J. Antimicrob. Chemother.* **72**, 2311–2319 (2017).